FtsK translocation permits discrimination between an endogenous and an imported Xer/*dif* recombination complex

Florian Fournes[a], Estelles Crozat[a], Carine Pages[a], Catherine Tardin[b], Laurence Salomé[b], François Cornet[a,1], and Philippe Rousseau[a,1]

[a]Laboratoire de Microbiologie et de Génétique Moléculaires (LMGM), Centre de Biologie Intégrative (CBI), Université de Toulouse, CNRS, Université Paul Sabatier, F-31062 Toulouse, France; and [b]Institut de Pharmacologie et de Biologie Structurale, Université de Toulouse, CNRS, Université Paul Sabatier, F-31062 Toulouse, France

Edited by Nancy E. Kleckner, Harvard University, Cambridge, MA, and approved April 18, 2016 (received for review November 23, 2015)

In bacteria, the FtsK/Xer/*dif* (chromosome dimer resolution site) system is essential for faithful vertical genetic transmission, ensuring the resolution of chromosome dimers during their segregation to daughter cells. This system is also targeted by mobile genetic elements that integrate into chromosomal *dif* sites. A central question is thus how Xer/*dif* recombination is tuned to both act in chromosome segregation and stably maintain mobile elements. To explore this question, we focused on pathogenic *Neisseria* species harboring a genomic island in their *dif* sites. We show that the FtsK DNA translocase acts differentially at the recombination sites flanking the genomic island. It stops at one Xer/*dif* complex, activating recombination, but it does not stop on the other site, thus dismantling it. FtsK translocation thus permits *cis* discrimination between an endogenous and an imported Xer/*dif* recombination complex.

XerCD | *dif* | FtsK | GGI | IMEX

In all organisms, the processing of chromosome ends or termini relies on specific activities for replication and segregation. In eukaryotes, telomeres are often targeted by mobile genetic elements, which may even substitute for telomeric functions (1). Circular chromosomes found in prokaryotes have no telomeres but harbor chromosome dimer resolution sites, called *dif* sites, on which dedicated Xer recombinases (XerC and XerD in most cases) act (2, 3). Besides their role in chromosome maintenance, *dif* sites are targeted by numerous mobile genetic elements, referred to as integrating mobile element exploiting Xer (IMEX) (4). How IMEXs integrate into *dif* without inactivating its cellular function and how they are stably maintained in their integrated state has remained unclear despite study over the past decade (4–7). Here we answer these questions by studying the gonococcal genomic island (GGI), an IMEX stably integrated into the *dif* site of pathogenic *Neisseria* species that encodes crucial functions for gene exchange and virulence (8, 9).

In *Escherichia coli*, chromosome dimers form by homologous recombination during replication and are resolved by site-specific recombination between sister *dif* sites catalyzed by the XerC and XerD recombinases (Fig. 1) (3). The 28-bp *dif* site carries binding sites for each recombinase, separated by a 6-bp central region at the border of which strand exchanges are catalyzed. After assembly of the recombination complex (synapse), one pair of strands is exchanged by the XerD monomers, leading to a branched DNA intermediate (Holliday junction, HJ) subsequently resolved by XerC. Dimer resolution is integrated into the general processing of the terminal region of the chromosome (*ter* region) during cell division (10). FtsK, a DNA translocase associated with the division apparatus, segregates this region at the onset of cell division (10, 11). The translocation motor, FtsKαβ, is located in the C terminal of FtsK (12). Translocation is oriented toward the *dif* site located at the center of the *ter* region via a direct interaction between the extreme C-terminal subdomain of FtsK, FtsKγ, and the KOPS DNA motifs (13). Upon reaching the XerCD/*dif* complex, FtsK stops translocating and activates recombination via direct interaction with XerD (14, 15) (Fig. 1). The mechanisms of translocation arrest and of recombination activation are poorly understood but they both involve FtsKγ. However, these activities appear to be distinct from each other because FtsKγ can activate recombination in vivo and in vitro when isolated from the FtsKαβ motor or fused to XerC or XerD (16).

In numerous bacteria, the XerCD/*dif* system is hijacked by IMEXs, which integrate their host genome into *dif* sites by using XerCD-mediated catalysis (4). In all of the reported cases, integration of IMEXs recreates a bona fide *dif* site, thereby not interfering with chromosome dimer resolution, which would lead to their counter-selection. The best-described examples are *Vibrio cholerae* IMEXs, which carry crucial virulence determinants (5–7, 17). These IMEXs have developed different strategies to integrate and to remain stably integrated, although the mechanisms ensuring their stable maintenance are not fully understood. *Neisseria* species contain an unusually long IMEX called the gonococcal genomic island (GGI) (8). In *Neisseria gonorrheae*, the GGI is 57 kb long and encodes a type IV secretion system that exports the chromosomal DNA of its host, rendering it available to neighboring cells for gene exchange by genetic transformation (8, 18). The GGI carries a *dif* site, dif_{GGI}, consisting of a XerC-binding site, a central region homologous to the *Neisseria dif* site, dif_{Ng}, and a divergent XerD-binding site (Fig. 1*B*). Comparison of *N. gonorrheae* strains harboring or lacking the GGI, together with functional data, indicates that the GGI integrates by XerCD-dependent recombination (9). The nonreplicative excised circular form of the GGI can be detected and the GGI can also be lost, showing that excision occurs, although at low frequencies (9). Although the GGI

Significance

This study focuses on a molecular machine (Xer/*dif*/FtsK) involved in circular chromosome processing during the bacterial cell cycle. Xer site-specific recombinases are well known to act at the chromosomal *dif* (dimer resolution) sites for chromosome dimer resolution (CDR). The Xer/*dif* recombination machine is, however, highly versatile and is also implicated in integration and excision of mobile genetic elements (MGE). Whereas CDR depends on the FtsK DNA translocase, MGE mobility somehow escapes this control. Focusing on the case of the gonococcal genetic island found in pathogenic *Neisseria* species, we reveal how FtsK distinguishes a Xer/*dif* complex involved in vertical genetic transfer (CDR) from one involved in horizontal gene transfer (MGE mobility).

Author contributions: F.F., E.C., F.C., and P.R. designed research; F.F., C.P., and P.R. performed research; F.F., E.C., C.T., and P.R. contributed new reagents/analytic tools; F.F., E.C., C.T., L.S., F.C., and P.R. analyzed data; and F.F., F.C., and P.R. wrote the paper.

The authors declare no conflict of interest.

This article is a PNAS Direct Submission.

Freely available online through the PNAS open access option.

[1]To whom correspondence may be addressed. Email: philippe.rousseau@ibcg.biotoul.fr or francois.cornet@ibcg.biotoul.fr.

This article contains supporting information online at www.pnas.org/lookup/suppl/doi:10.1073/pnas.1523178113/-/DCSupplemental.

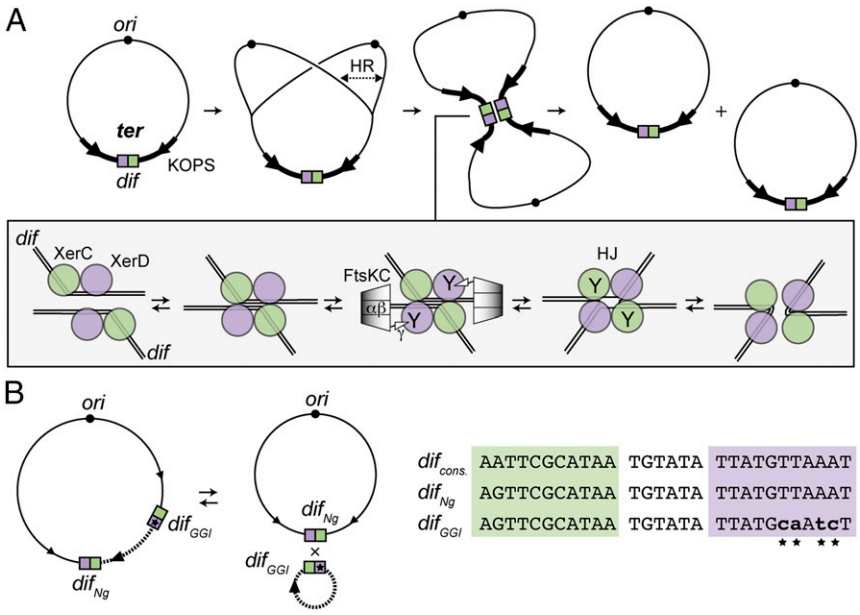

Fig. 1. The XerCD/*dif* recombination. (*A*) Chromosome dimer formation by homologous recombination (HR) during replication and resolution by site-specific recombination between the two *dif* sites. The *dif* site is represented as green and purple boxes for the XerC-binding and the XerD-binding sites, respectively. ori (black circle), some KOPS motifs (arrows), and the *ter* domain (thick line) are represented. The mechanism of XerCD/*dif* recombination is represented in the box. XerC (green circles) and XerD (purple circles) bind two distant *dif* sites to create a synapse. Hexamers of the FtsK C-terminal domain [FtsKC: FtsKαβ: (diamonds) + FtsKγ: (triangle) contacting XerD] translocate toward *dif* and contact XerD. This activates XerD (Y indicates the active recombinases), which catalyzes the first-strand exchange. This process leads to the formation of an HJ intermediate within which XerC is active and catalyzes the second-strand exchange (3). (*B*) Integration and excision of the GGI (dotted line) by XerCD catalysis. KOPS, dif_{Ng}, and dif_{GGI} sites are represented as in *A*. An alignment of dif_{Ng}, dif_{GGI} and consensus *dif* sequence (27, 28) is shown on the left. Substituted positions in dif_{GGI} are represented as lowercase characters and highlighted by stars.

was identified over a decade ago, it has remained unclear how DNA flanked by two Xer recombination sites is stably maintained at a chromosomal locus processed by FtsK during each cell cycle. In this study, we have combined in vitro and in vivo approaches to show that dif_{GGI} is indeed an active Xer recombination site at which the *Neisseria* Xer recombinases catalyze recombination when activated by FtsKγ. However, we find that recombination between dif_{Ng} and dif_{GGI} is inhibited by translocating FtsK. Inhibition is a result of the absence of translocation arrest at $XerCD_{Ng}/dif_{GGI}$ complexes that most likely precludes recombination activation, an absence that causes the complex to dismantle. We conclude that, depending on the sequence of the recombination site, Xer recombination complexes have the intrinsic capacity to be activated or inhibited by FtsK.

Results

Xer Recombination Complexes Readily Form at dif_{Ng} and dif_{GGI}. *N. gonorrheae* encodes XerC and XerD homologs as well as two FtsK homologs (19). We cloned and purified tagged versions of $XerC_{Ng}$ and $XerD_{Ng}$ (*Methods*, *SI Text*, and Fig. S1*A*) and used the two proteins in EMSA experiments. $XerC_{Ng}$ or $XerD_{Ng}$ alone formed two complexes with either radiolabeled dif_{Ng}, or dif_{GGI} (Fig. 2, *SI Text*, and Fig. S1 *B* and *C*). Comparison with results from the *E. coli* Xer system suggests that the first complex corresponds to the binding of one recombinase monomer (*dif*-Xer), and the second to the binding of two recombinases monomers to both sides of the recombination sites (*dif*-Xer^2) (20). The ratios of these two complexes were different between the dif_{Ng} and dif_{GGI} sites (*SI Text* and Fig. S1 *B* and *C*). However, the overall efficiency of either $XerC_{Ng}$ or $XerD_{Ng}$ binding was similar on the two sites. As in the case in *E. coli*, $XerC_{Ng}$ and $XerD_{Ng}$ bound cooperatively to dif_{Ng} (Fig. 2*B* and Fig. S1*E*). Similar efficiencies of complex formation were obtained with dif_{GGI} (Fig. 2*D* and Fig. S1*E*). We concluded that $XerD_{Ng}$ readily binds to dif_{GGI} despite the four base changes of its predicted binding site compared with dif_{Ng} (Fig. 1). In addition, $XerCD_{Ng}/dif_{GGI}$ complexes formed as efficiently as $XerCD_{Ng}/dif_{Ng}$ complexes by cooperative binding of the two recombinases.

Once assembled, XerCD-*dif* complexes come together in a recombination-proficient complex containing two monomers of each recombinase gathering two recombination sites (Fig. 1*A*). We used tethered particle motion (TPM) (21, 22), a single-molecule technique that involves tracking beads attached at one end of the DNA molecules while the other extremity of the DNA is tethered to a coverslip (*Methods* and Fig. 3*A*). The amplitude of motion at equilibrium of the bead (Aeq) directly depends on the apparent length of the DNA (22, 23). We constructed two 2,311-bp long DNA molecules, containing either two dif_{Ng} sites or a dif_{Ng} and a dif_{GGI} site separated by 945 bp, and recorded their Aeq with a recently developed multiplexed version of the TPM [high-throughput (HT)-TPM] (*Methods* and Fig. 3*A*) (22). Addition of $XerC_{Ng}$ and $XerD_{Ng}$ to either DNA molecule resulted in a displacement toward smaller values and a broadening of Aeq distribution well fitted by two Gaussian peaks (Fig. 3*B*, *Right*). The first peak (I: 70% of the probability density) was shortened by 10 nm compared with the naked DNA. This shortening was too small to be a result of formation of a recombination complex and was more likely because of $XerD_{Ng}$ binding to the recombination sites, as

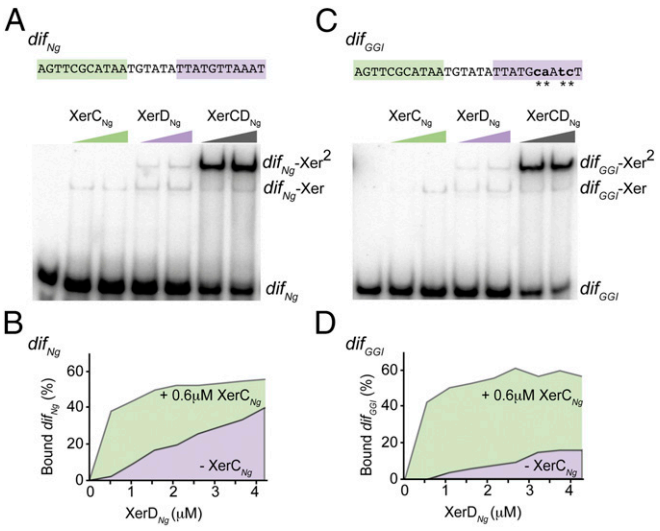

Fig. 2. $XerC_{Ng}$ and $XerD_{Ng}$ bind to dif_{Ng} and dif_{GGI}. EMSA experiment showing the interaction between an increasing concentration of $XerC_{Ng}$ (0.4 and 0.6 μM) and $XerD_{Ng}$ (1.4 and 1.8 μM) and a 28-bp DNA fragment containing either dif_{Ng} (*A*) or dif_{GGI} (*C*). The color code used is the same as in Fig. 1. Unbound DNA (*dif*), complexes with one recombinase bound (*dif*–Xer), and complexes with two recombinases bound (*dif*–Xer^2) are represented. In *C*, substituted positions in dif_{GGI} are represented as lowercase characters and highlighted by stars. (*B* and *D*) Titration experiment of dif_{Ng} (*B*) or dif_{GGI} (*D*) by $XerD_{Ng}$. The experiment was done in presence (underlined with green) or in absence (underlined with purple) of $XerC_{Ng}$ (see also Fig. S1*E*).

previously observed with *E. coli* XerD (21). The second peak (II: 30% of the probability density) was shortened by 60 nm. Considering the TPM calibration equation [ΔAeq (in nm) = 0.0623 L (in bp) + 92.3; measured in these very same experimental conditions (21)], this shortening was consistent with the formation of a recombination complex (Aeq = 0.0623 × 945 ~ 59 nm). No difference was detected between the DNA containing either two dif_{Ng} or one dif_{Ng} and one dif_{GGI} (Fig. 3 *B* and *C*). We concluded that $XerC_{Ng}$ and $XerD_{Ng}$ form recombination complexes between dif_{Ng} sites. Most importantly, equivalent complexes also formed between dif_{Ng} and dif_{GGI}, suggesting that the base changes present in dif_{GGI} do not affect the formation of recombination complexes.

Both dif_{Ng} and dif_{GGI} Are Active Xer Recombination Sites. To directly monitor recombination, we constructed two reporter-cassettes, dif_{Ng}-dif_{Ng} and dif_{Ng}-dif_{GGI}, containing a kanamycin-resistance gene between the two *dif* sites, and inserted them on a plasmid (Fig. 4*A*). In vitro assays performed by incubating the dif_{Ng}-dif_{Ng} plasmid with $XerC_{Ng}$ and $XerD_{Ng}$ resulted in the appearance of a faint quantity of branched DNA containing a HJ [Fig. 4*B*, *Left* (*Center* column); see *SI Text* and Fig. S2 for HJ characterization], an intermediate in Xer recombination (16). These HJ-containing forms were not detected with the dif_{Ng}-dif_{GGI} plasmid [Fig. 4*C*, *Left* (*Center* column)]. We next constructed a constitutively active version of $XerD_{Ng}$, $XerD\gamma_{Ng}$, by fusing the FtsKγ subdomain of *N. gonorrheae* to the C terminus of $XerD_{Ng}$ (*Methods* and Figs. S1 *A* and *D* and S2) (16). Substituting $XerD_{Ng}$ for $XerD\gamma_{Ng}$ yielded increased levels of HJ and recombination products for both dif_{Ng}-dif_{Ng}– and dif_{Ng}-dif_{GGI}–containing plasmids [Fig. 4 *B* and *C*, *Left* (*Right* columns)]. In these reactions, $XerD\gamma_{Ng}$ likely catalyzes the initial strand exchange because the HJ were not detected using a catalytically inactive variant of this protein (*SI Text* and Fig. S2). We conclude that $FtsK\gamma_{Ng}$ activates Xer recombination by activating $XerD_{Ng}$-mediated catalysis and that $FtsK\gamma_{Ng}$ can activate recombination between dif_{Ng} and dif_{GGI} to the same level as recombination between dif_{Ng} sites.

To assess the activity of $XerCD_{Ng}$ in vivo, we then placed these reporter cassettes into the *E. coli* chromosome in place of the natural *dif* site (*Methods* and Fig. 4*A*). In the strains carrying the cassettes on their chromosome, the endogenous *xerC* gene was replaced by $xerC_{Ng}$, whereas the endogenous *xerD* was deleted (*Methods*). Recombination was induced by transformation with a plasmid containing $xerD_{Ng}$ under the control of an arabinose-inducible promoter (*Methods*). In *E. coli*, $XerC_{Ng}$ and $XerD_{Ng}$ promoted recombination between dif_{Ng} sites, which partly depended on *E. coli* FtsK ($FtsK_{Ec}$) (Fig. 4*B*, *Right*). Recombination was increased and became independent of $FtsK_{Ec}$ when $XerD_{Ng}$ was replaced with $XerD\gamma_{Ng}$ (Fig. 4*B*, *Right*). Recombination between dif_{Ng} and dif_{GGI} differed from dif_{Ng}-dif_{Ng} recombination in several ways. Recombination was barely detected between dif_{Ng} and dif_{GGI} with $XerC_{Ng}$ and $XerD_{Ng}$ (Fig. 4*C*, *Right*), consistent with the absence of the HJ in vitro (Fig. 4*C*, *Left*). Recombination between dif_{Ng} and dif_{GGI} is thus less efficient than recombination between two dif_{Ng}. Substituting $XerD_{Ng}$ by $XerD\gamma_{Ng}$ increased recombination, showing that, as observed in vitro (Fig. 4*C*, *Right*), the *Neisseria* $FtsK\gamma_{Ng}$ domain activates recombination between dif_{Ng} and dif_{GGI}. This finding confirms that dif_{GGI} is an active site that recombines with dif_{Ng} when activated by $FtsK\gamma_{Ng}$.

The FtsKC Motor Inhibits GGI Excision. Surprisingly, $XerC_{Ng}$-$XerD\gamma_{Ng}$ catalyzed recombination between dif_{Ng} and dif_{GGI} strongly increased in a strain deleted for the whole C-terminal part of $FtsK_{Ec}$ ($FtsK\alpha\beta\gamma_{Ec}$) (Fig. 4*C*, *Right*) (ΔC) and reached frequencies equivalent to those of the dif_{Ng}-dif_{Ng} recombination in the same strain (compare Fig. 4 *B* and *C*, *Right*). Thus, the whole *E. coli* FtsK C-terminal domain ($FtsKC_{Ec}$) inhibits dif_{Ng}-dif_{GGI} recombination in these conditions. This observation prompted us to explore the effect of the C-terminal part of *Neisseria* FtsK ($FtsKC_{Ng}$) on $XerC_{Ng}$-$XerD\gamma_{Ng}$–driven recombination between dif_{Ng} and dif_{GGI}. Production of $FtsKC_{Ng}$ from a plasmid in an otherwise ΔC strain (*SI Text* and Fig. S3) yielded 27% inhibition of $XerC_{Ng}$ and $XerD\gamma_{Ng}$ catalyzed recombination between dif_{Ng} and dif_{GGI} (Fig. S3). $FtsKC_{Ng}$ thus

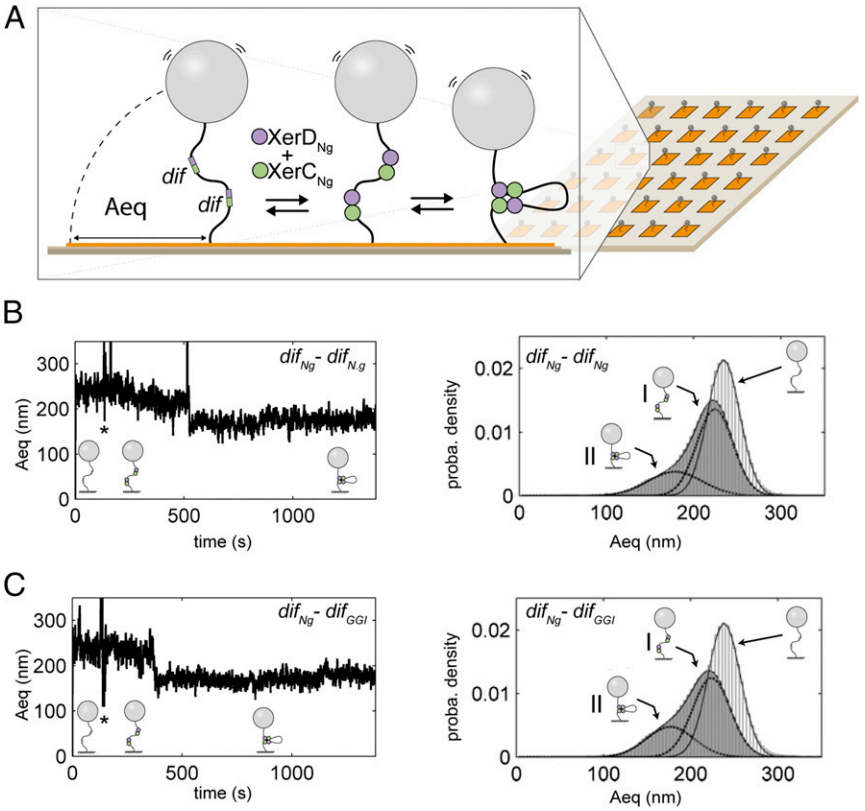

Fig. 3. HT-TPM measurement of recombination complex formation. (*A*) A glass coverslip (pale brown) is coated with neutravidin (orange). A DNA molecule is attached to this surface by biotin bound to one of its 5′ end. A latex bead coated with anti-digoxigenin is bound to the other extremity of the DNA carrying digoxigenin at its 5′ end. $XerC_{Ng}$ and $XerD_{Ng}$ (green and purple circles) bind *dif* sites (green and purple boxes) and the formation of a complex between two *dif* sites significantly decreases the amplitude of bead motion (Aeq). (*B* and *C*, *Left*) Typical traces [Aeq = *f*(time)] observed for DNA molecules containing either two dif_{Ng} sites (*B*) or one dif_{Ng} one dif_{GGI} sites (*C*). Stars (*) indicate the times of $XerCD_{Ng}$ mix injection. Schemes of the inferred DNA structures of the DNA are shown underneath each trace. (*Right*) Probability distributions of Aeq before protein addition (light gray) and during the 20 min following $XerCD_{Ng}$ addition (dark gray). The Gaussian fitting curves, used to characterize the different DNA subpopulations contributing to the Aeq distributions, are superimposed to the distributions as well as the schemes of the inferred DNA structures for each subpopulation (I refers to the first peak and II to the second).

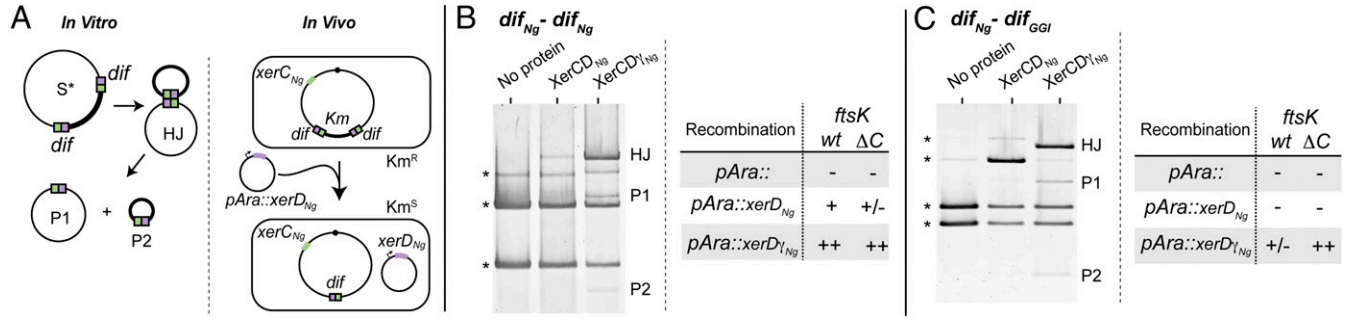

Fig. 4. In vivo and In vitro GGI excision. (*A*) Schemes of the in vitro (*Left*) and in vivo (*Right*) assays used. The color code is as in Fig. 1. (*B*) In vitro recombination reactions using plasmids containing the dif_{Ng}-dif_{Ng} cassette. After DNA restriction, substrate (*) and products (HJ, P1, and P2) are separated by electrophoresis. In vivo recombination reactions using *E. coli* strains containing the dif_{Ng}-dif_{Ng} cassette inserted at the *dif* locus. Recombination was scored as the appearance of kanamycin-sensitive colonies after production of either $XerD_{Ng}$ or $XerD\gamma_{Ng}$. The experiment was done in *wt* and Δ*C ftsK* strains (*Methods*). –, Less than 2%; ±, 2–10%; +, 10–50%; ++, 50–100% kanamycin colonies (see also Table S1). (*C*) Same as *B* but for dif_{Ng}-dif_{GGI} cassettes.

inhibited recombination between dif_{Ng} and dif_{GGI}, although to a lower extent compare with $FtsK_{Ec}$. This difference might be because of a poor activity of $FtsKC_{Ng}$ in these conditions. Importantly, recombination between two dif_{Ng} sites was neither inhibited by $FtsK_{Ec}$ nor by $FtsKC_{Ng}$. This result shows that FtsKC specifically inhibits recombination between the dif_{Ng} and dif_{GGI} sites.

To assay the role of the FtsK motor in vitro, we used purified trimeric $FtsK\alpha\beta\gamma_{Ec}$ (t-$FtsK\alpha\beta\gamma_{Ec}$) constructed from *E. coli* FtsK, which is known to translocate efficiently (24). We also used linear instead of supercoiled DNA substrates to lower the efficiency of recombination and ease the detection of inhibitory effects (*Methods* and Fig. 5*A*). In these conditions, both dif_{Ng}-dif_{Ng} and the dif_{Ng}-dif_{GGI} reporter cassettes formed HJ intermediates in equivalent amounts in the presence of $XerC_{Ng}$ and $XerD\gamma_{Ng}$ but no complete duplex products were detected (Fig. 5*B*). Addition of t-$FtsK\alpha\beta\gamma_{Ec}$ and ATP to reactions containing $XerC_{Ng}$ and $XerD\gamma_{Ng}$ did not alter HJ formation between dif_{Ng} sites (Fig. 5*B*, *Left*). Conversely, addition of t-$FtsK\alpha\beta\gamma_{Ec}$ lowered HJ quantity detected between dif_{Ng} and dif_{GGI} (Fig. 5*B*, *Right*). This effect was ATP-dependent (Fig. 5*B* and Fig. S4*A*), suggesting it was caused by the translocation activity of t-$FtsK\alpha\beta\gamma_{Ec}$. Although we cannot completely exclude that t-$FtsK\alpha\beta\gamma_{Ec}$ stimulates HJ resolution back to its initial substrate form, we inferred that t-$FtsK\alpha\beta\gamma_{Ec}$ inhibits HJ formation. Taken together, these results strongly suggest that recombination between dif_{Ng} and dif_{GGI} is inhibited by the translocase activity of t-$FtsK\alpha\beta\gamma_{Ec}$.

FtsK Translocation Stops on $XerCD_{Ng}$/dif_{Ng} but Not on $XerCD_{Ng}$/dif_{GGI}. FtsK is a powerful translocase able to displace proteins bound to DNA in vitro (14, 15). In contrast, FtsK specifically stops on XerCD/*dif* complexes, which is likely a prerequisite for the activation of recombination (14–16, 25). Because FtsK appears to inhibit the first steps of recombination between dif_{Ng} and dif_{GGI}, we tested its capacity to stop translocating when encountering $XerCD_{Ng}$/dif_{GGI} complexes. We took advantage of the fact that t-$FtsK\alpha\beta\gamma_{Ec}$ translocation was shown to break a biotin–streptavidin link placed at the end of a DNA molecule (24). One extremity of a DNA molecule containing a recombination site (dif_{Ng} or dif_{GGI}) was attached to a magnetic bead by a biotin/streptavidin link. t-$FtsK\alpha\beta\gamma_{Ec}$ should only break the biotin/streptavidin link and dissociate the DNA from the bead if a XerCD/*dif* complex was unable to stop translocation (Fig. 6*A*). The quantity of free DNA yielded after t-$FtsK\alpha\beta\gamma_{Ec}$ action is thus inversely proportional to the capacity of a XerCD/*dif* complex to stop translocation. Results are shown in Fig. 6*B*, with the total DNA (after heat denaturation) presented beside the free DNA recovered in the supernatant after magnetic pull-down. Incubation of the DNA-bead complexes with t-$FtsK\alpha\beta\gamma_{Ec}$ (and ATP) led to an increase in the quantity of free DNA recovered compared with incubation with $XerCD_{Ng}$. Dissociation of the DNA–bead complexes depended on the concentration of t-$FtsK\alpha\beta\gamma_{Ec}$ and ATP, suggesting that it is a result of translocation of t-$FtsK\alpha\beta\gamma_{Ec}$ (*SI Text* and Fig. S4*B*). Addition of $XerC_{Ng}$ and $XerD_{Ng}$ in absence of t-$FtsK\alpha\beta\gamma_{Ec}$ did not dissociate the DNA–bead complexes (Fig. 6*B*). When $XerC_{Ng}$, $XerD_{Ng}$, and t-$FtsK\alpha\beta\gamma_{Ec}$ were incubated together with the dif_{Ng}-containing DNA–bead complexes, the quantity of free DNA decreased, showing that t-$FtsK\alpha\beta\gamma_{Ec}$ translocation stops at $XerCD_{Ng}$/dif_{Ng} complexes (Fig. 6*B*). The difference of free DNA recovered in the absence and in the presence of the recombinases (percent protection) (Fig. 6*B*) showed significant although not total arrest of FtsK. This result is consistent with the binding experiment (Fig. 2), which did not show 100% dif_{Ng} binding by $XerCD_{Ng}$, and with previous FtsK arrest experiments (14). This protection effect was independent of the orientation of the dif_{Ng} site (i.e., FtsK reaching the $XerCD_{Ng}$/dif_{Ng} complex by its $XerC_{Ng}$ or $XerD_{Ng}$ side) (Fig. S4*C*). In contrast to this finding, incubation of $XerC_{Ng}$, $XerD_{Ng}$, and t-$FtsK\alpha\beta\gamma_{Ec}$ with dif_{GGI}-containing DNA–bead

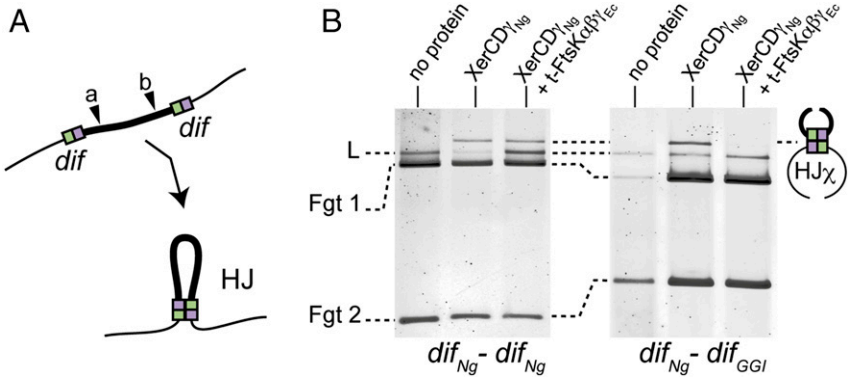

Fig. 5. In vitro HJ formation. (*A*) Schematic of the in vitro HJ formation assay using a color code as in Fig. 1. NcoI restriction site is represented: (*a*) for dif_{Ng}-dif_{Ng} cassette and (*b*) for dif_{Ng}-dif_{GGI} cassette. (*B*) HJ formation for dif_{Ng}-dif_{Ng} (*Left*) or dif_{Ng}-dif_{GGI} (*Right*) cassettes. As indicated, DNA substrates were incubated with $XerD_{Ng}$ and $XerD\gamma_{Ng}$ ± t-$FtsK\alpha\beta\gamma_{Ec}$. After DNA restriction, $HJ\chi$ were separated from substrate DNA by electrophoresis: linear (L, partial restriction) and fragments (Fgt 1 and Fgt 2, total restriction).

complexes did not alter levels of free DNA compared with incubation with t-FtsKαβγ_{Ec}, suggesting that t-FtsKαβγ_{Ec} did not stop at dif_{GGI} recombination complexes (Fig. 6*B*). Again, the orientation of the dif_{GGI} site was unimportant (Fig. S4*C*). We conclude that XerCD$_{Ng}$/dif_{GGI} complexes cannot stop t-FtsKαβγ_{Ec} translocation efficiently and are thus dissociated by t-FtsKαβγ_{Ec}. These results may explain how t-FtsKαβγ_{Ec} inhibited HJ formation between dif_{Ng} and dif_{GGI} but not between two dif_{Ng} (Fig. 5*B*). Indeed, it is tempting to postulate that t-FtsKαβγ_{Ec} dissociates XerCD$_{Ng}$/dif_{GGI} complexes before HJ formation.

Discussion

Mobile genetic elements need to accurately balance their stability and transfer. This is most pertinent in the case of IMEXs that use the host Xer machine for mobility. Indeed, FtsK may induce Xer recombination between *dif* sites at each generation. Consistent with this view, segregation of the region surrounding the *dif* site is accomplished by FtsK, whether the chromosomes are dimeric or monomeric (10). IMEXs are nevertheless rarely excised and lost. The GGI is present in 80% of *N. gonorrheae* strains and the excised form is barely detected (8, 9). We have shown here that the integrated form of the GGI is flanked by two active Xer sites. Recombination between these sites is induced by the FtsKγ_{Ng} activating domain, with XerD$_{Ng}$ mediating exchange of the first pair of strands as in the resolution of chromosome dimers. This finding suggests that a classic FtsK-controlled XerCD/*dif* reaction promotes GGI excision, which should thus be very efficient. However, recombination is not activated when a translocation-proficient form of FtsK is added (either FtsK$_{Ec}$ or FtsKC$_{Ng}$ in vivo or t-FtsKαβγ_{Ec} in vitro) (Figs. 4 and 5). We resolved this apparent paradox by showing that the dif_{GGI} site, bound by Xer recombinases, is not recognized as a bona fide *dif* site by the FtsK motor. Indeed, the XerCD$_{Ng}$/dif_{GGI} complex does not stop t-FtsKαβγ_{Ec} translocation; this most probably leads to disassembly of the complex and precludes recombination activation. Such an unsuspected level of control by which FtsK activates or represses Xer recombination in response to subtle changes in the recombination complex provides a clue to the question of how GGI-type IMEXs can be stably maintained in host *dif* sites.

The *Neisseria* Xer recombinases and *dif* site, dif_{Ng}, function similarly to their *E. coli* counterparts. The XerCD$_{Ng}$/dif_{Ng} complex can form HJs but no complete duplex recombination products. Complete recombination requires FtsKγ_{Ng} (Fig. 4). *E. coli* FtsK can activate XerCD$_{Ng}$/dif_{Ng} recombination, although inefficiently, suggesting that activation is partly species-specific, as previously reported for *E. coli* and *Haemophilus influenzae* (26). The dif_{GGI} site differs from dif_{Ng} at four positions all included in the XerD-binding site (Fig. 1*B*). These positions correspond to variable positions in the *dif* consensus (27, 28) and do not preclude the assembly of a recombination complex that can be activated for catalysis by FtsKγ_{Ec} (Figs. 2–4). Clearly, the XerCD$_{Ng}$/dif_{GGI} complex assembles with the same efficiency as the XerCD$_{Ng}$/dif_{Ng} complex. In addition, these two complexes form recombination complexes as efficiently as two XerCD/dif_{Ng} complexes. These findings may appear surprising, given the high conservation of the XerD-binding sites of *dif* sites, suggesting a particular selection pressure on the sequence of this part of *dif* (27, 28). However, we show that XerCD$_{Ng}$/dif_{GGI} complexes do not stop t-FtsKαβγ_{Ec} translocation. The selection pressure on the XerD-binding site may then reside in the capacity of the *dif* site to assemble a complex able to stop FtsK, which would require a particular interaction of XerD with its binding site involving bases not directly involved in catalysis. Using single-molecule FRET, it has recently been shown that XerCD/*dif* complexes may adopt different conformations (25). The nucleotides modified within dif_{GGI} may favor one of these conformations that would not be recognized by FtsK.

Following KOPS directionality, FtsK preferentially translocates toward *dif* (13, 15). Translocation is powerful enough to strip bound proteins off DNA (14, 15). Recent experiments using t-FtsKαβγ_{Ec} reported that the stripping efficiency and outcome depends on the affinity for DNA of the protein to displace (15). The stripping activity is proposed to have functional implications in releasing MatP/*matS*-mediated cohesion between the *ter* regions of the sister chromosome during cytokinesis in *E. coli* (10). Exceptions to the stripping effect are XerCD/*dif* complexes, whether they are synapsed or not, at which t-FtsKαβγ_{Ec} stops and resides for a very short time, during which a single round of recombination can be induced (25). Our results suggest an additional role of the stripping activity in stabilizing IMEXs. In these cases, FtsK would inhibit excision by dismantling the recombination complexes assembled at one of the *dif* sites flanking the IMEX. The stoppage or stripping-off choice thus appears crucial in differentiating chromosome dimer resolution sites from other Xer sites.

The recombination activation activity of FtsK can be separated from translocation, for example by fusing FtsKγ to XerD. However, translocation appears to be a prerequisite for activation in the natural situation (i.e., when FtsKγ is linked to the FtsK motor). This can be inferred from the incapacity of FtsK mutants defective in translocation (i.e., unable to hydrolyze ATP) to induce recombination (29, 30). We further show that an active FtsK motor also fails to activate recombination if unable to stop at the recombination complex. This failure can be observed in vitro and in vivo even when recombination is constitutively activated using a XerD–FtsKγ fusion (Figs. 4 and 5). Thus, both translocation and programmed stoppage are required for the activation of recombination, providing a tight control of this process.

The rapidly increasing number of known IMEXs have been classified following the structure of the Xer site they carry, specifying types of integration and excision mechanisms (4). These Xer sites carry at least an intact binding site, either for XerC or for XerD, resulting in the reformation of an active chromosome dimer resolution site after integration, which guarantees that integration is harmless for chromosome segregation. Excision then needs to be prohibited or tightly controlled. Most described IMEXs use a mechanism involving first-strand exchange by XerC without a catalytic role for XerD, thereby escaping activation by FtsK. The GGI, as well as the *V. cholerae* IMEX, called TLC (6), do not follow this paradigm but use a chromosome dimer resolution-like mechanism, with XerD exchanging the first pair of strands followed by XerC catalysis. In the case of the GGI, FtsK directly inhibits excision by stripping off the recombinases from one of the two *dif* sites. The Xer recombination complexes thus have the intrinsic capacity to be activated or inhibited by FtsK depending on the sequence of the recombination site. Understanding the molecular basis of this dual control urgently calls for structural studies of the Xer recombination machine.

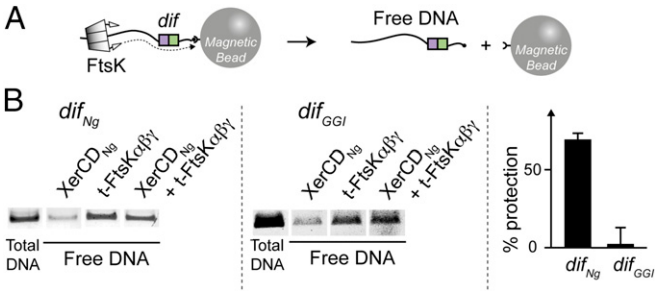

Fig. 6. FtsK stoppage on XerCD/*dif* complexes. (*A*) Schematic of the translocation assay using a color code as in Fig. 1. The dotted line represents FtsK translocation, which releases the DNA from the bead (biotine/streptavidin link breakage), allowing its recovery in the bead-free supernatant after bead pull down (*Methods*). (*B*) Each gel represents the analysis of free DNA obtained after incubation of the substrate (DNA containing dif_{Ng} or dif_{GGI}) with XerCD$_{Ng}$, t-FtsKαβγ_{Ec} or both. The "total DNA" control was obtained by heat denaturation of the different DNA-bead complexes. The "% protection" represents the difference of free DNA obtained after t-FtsKαβγ_{Ec} incubation in absence and presence of XerCD$_{Ng}$ (mean of at least three independent experiments with SDs).

Methods

Strain and Plasmids. *N. gonorrheae* $xerC_{Ng}$ and $xerD_{Ng}$ genes (NGO0035 and NGO0329), were synthesized by Genscript and cloned in pET32b (Navagen) to give pROUT008 and pROUT011 plasmids. PROUT008 was used to construct $xerD\gamma_{Ng}$ (pFF011). *N. gonorrheae* $xerC_{Ng}$ and $xerD_{Ng}$ genes were also cloned into pBAD18 to give the pCP127 and pCP128, respectively, and pCP128 was used to introduce $xerD\gamma_{Ng}$ into pBAD18 (pFF013). For in vitro analysis, synthetic Kanamycin-resistant cassettes (pFF01: dif_{Ng}-Kn-dif_{Ng}, pFF03: dif_{Ng}-Kn-dif_{GGI}) were generated on pUC57 and transferred into *E. coli* (DS941: AB1157*recF143 lacIq* Δ*(lacZ)M15*). In *E. coli* CP1088 [LN2666: W1485 F-*leu thyA thi deoB or C supE rpsl* (StR); *xerD::frt*; *xerC::frt*], the *dif* site was substituted by one of the two possible cassettes, using a previously described insertion/deletion procedure (31) (CP1106, CP1108). To produce $XerC_{Ng}$ in these strains, $xerC_{Ng}$ was inserted at the *xerC::frt locus* (31): CP1182 (CP1106, $xerC_{Ng}$); CP1184 (CP1108, $xerC_{Ng}$). To produce $XerD_{Ng}$ or $XerD\gamma_{Ng}$, these strains were transformed by pBAD18 derivatives carrying $xerD_{Ng}$ or $xerD\gamma_{Ng}$.

Protein Purification. Expression plasmids (pROUT008 or pROUT011 or pFF011) were used to transform the *E. coli* BL2-DE3 strain. Xer proteins were purified as described previously (21). The purification of t-FtsK$\alpha\beta\gamma_{Ec}$ was performed as in ref. 24.

EMSA. The 28-bp 5′-end-labeled [γ^{32}P] DNA fragments carrying dif_{Ng} and dif_{GGI} sites were used in a binding reaction carried out as in ref. 32 and analyzed with a typhoon TRIO GE.

Multiplexed Tethered Particle Motion Analysis. The overall HT-TPM procedure, including data analysis, has been described previously (22, 33). The 2,311-bp long DNA molecules were produced by PCR from pFF01, pFF03, and purified as previously described (21). Data acquisitions were performed at 22 °C for 25 min. The initial step of 2 min corresponds to the tracking of the DNA–beads complexes in the reaction buffer (10 mM Tris·HCl pH 8, 160 mM NaCl, 1 mM $MgCl_2$, and 1 mg/mL Pluronic F-127). It is followed by the injection of a mix of 50 nM $XerD_{Ng}$ and 50 nM $XerC_{Ng}$ diluted in the same buffer.

Recombination Assays. In vivo recombination experiments were performed using CP1182, or CP1184 strains transformed with pCP128 or pFF03, as previously described (32). In vitro recombination reactions were performed as previously described (16). The final concentration of each Xer protein was 0.8 μM. The concentration of substrate plasmid used was 300 ng per reaction. After 1 h at 30 °C, phenol/chloroform extraction and ethanol precipitation, products were digested by NcoI and ScaI (Fermentas), analyzed on 0.8% agarose gels, and visualized by Sybr Green coloration using Typhoon-Trio-GE. For HJ detection, 50 ng of linear DNA [NdeI (Fermentas) digestion of pFF01 or pFF03] was incubated with proteins (160 nM $XerC_{Ng}$ + 160 nM $XerD\gamma_{Ng}$ ± 1 μM t-FtsK$\alpha\beta\gamma_{Ec}$) in a buffer containing 25 mM Tris·HCl pH 7.5, 10 mM $MgCl_2$, 0.5% glycerol, 0.02 mM EDTA, 0.02 mM DTT, 0.1% PEG 8000, 75 mM NaCl, and 6.25 mM ATP. After incubation at room temperature for 20 min, DNA was purified as described for the in vitro recombination assay (see above), digested by NcoI (Fermentas), and finally analyzed as described for the in vitro recombination assay (see above).

Translocation Test. DNA molecules were obtained by PCR on pFF01 or pFF02. These DNA molecules were mixed with streptavidin-coated magnetic beads (Streptavidin MagneSphere, Promega), at a ratio of 15 ng of DNA for 1 mL of the commercial beads solution, in 25 mM Tris·HCl pH 7.5, 10 mM $MgCl_2$ buffer. After 30-min incubation at room temperature, beads were precipitated and washed to eliminate most unbound DNA. Translocation reactions were carried out in 25 mM Tris·HCl pH 7.5, 10 mM $MgCl_2$, 10% (vol/vol) glycerol, 2 mM EDTA, 2 mM DTT, 250 mM NaCl, 5 mM ATP. Reactions contained 45 ng of DNA and 500 nM of each protein present: t-FtsK$\alpha\beta\gamma_{Ec}$ and/or $XerD_{Ng}$ and $XerC_{Ng}$. Reactions were incubated at room temperature for 1 min and beads were precipitated. Supernatant was collected and placed at 42 °C for 15 min with buffer containing 10% SDS, 2 mg/mL proteinase K, 0.01 mg/mL biotin. Products were analyzed by electrophoresis, as described above.

ACKNOWLEDGMENTS. We thank all the members of our teams, F.-X. Barre, and C. Midonet for helpful discussions; M. Sahli and B. Laisnez for technical assistance; A. Segall for providing peptides; and C. Johnston for help with the manuscript. This work was funded by the CNRS, University of Toulouse 3–Paul Sabatier and ANR Contracts 11NANO01003 and 14CE10000701; and a fellowship from the "Ministère de l'Enseignement Supérieur et de la Recherche" (to F.F.).

1. Levin HL, Moran JV (2011) Dynamic interactions between transposable elements and their hosts. *Nat Rev Genet* 12(9):615–627.
2. Blakely G, et al. (1993) Two related recombinases are required for site-specific recombination at *dif* and *cer* in *E. coli* K12. *Cell* 75(2):351–361.
3. Crozat E, Fournes F, Cornet F, Hallet B, Rousseau P (2014) Resolution of multimeric forms of circular plasmids and chromosomes. *Microbiol Spectr* 2(5).
4. Das B, Martínez E, Midonet C, Barre F-X (2013) Integrative mobile elements exploiting Xer recombination. *Trends Microbiol* 21(1):23–30.
5. Bischerour J, Spangenberg C, Barre F-X (2012) Holliday junction affinity of the base excision repair factor Endo III contributes to cholera toxin phage integration. *EMBO J* 31(18):3757–3767.
6. Midonet C, Das B, Paly E, Barre F-X (2014) XerD-mediated FtsK-independent integration of TLCϕ into the *Vibrio cholerae* genome. *Proc Natl Acad Sci USA* 111(47):16848–16853.
7. Val M-E, et al. (2005) The single-stranded genome of phage CTX is the form used for integration into the genome of *Vibrio cholerae*. *Mol Cell* 19(4):559–566.
8. Dillard JP, Seifert HS (2001) A variable genetic island specific for *Neisseria gonorrhoeae* is involved in providing DNA for natural transformation and is found more often in disseminated infection isolates. *Mol Microbiol* 41(1):263–277.
9. Domínguez NM, Hackett KT, Dillard JP (2011) XerCD-mediated site-specific recombination leads to loss of the 57-kilobase gonococcal genetic island. *J Bacteriol* 193(2):377–388.
10. Stouf M, Meile J-C, Cornet F (2013) FtsK actively segregates sister chromosomes in *Escherichia coli*. *Proc Natl Acad Sci USA* 110(27):11157–11162.
11. Crozat E, Rousseau P, Fournes F, Cornet F (2014) The FtsK family of DNA translocases finds the ends of circles. *J Mol Microbiol Biotechnol* 24(5-6):396–408.
12. Löwe J, et al. (2008) Molecular mechanism of sequence-directed DNA loading and translocation by FtsK. *Mol Cell* 31(4):498–509.
13. Bigot S, et al. (2005) KOPS: DNA motifs that control *E. coli* chromosome segregation by orienting the FtsK translocase. *EMBO J* 24(21):3770–3780.
14. Graham JE, Sivanathan V, Sherratt DJ, Arciszewska LK (2010) FtsK translocation on DNA stops at XerCD-*dif*. *Nucleic Acids Res* 38(1):72–81.
15. Lee JY, Finkelstein IJ, Arciszewska LK, Sherratt DJ, Greene EC (2014) Single-molecule imaging of FtsK translocation reveals mechanistic features of protein-protein collisions on DNA. *Mol Cell* 54(5):832–843.
16. Grainge I, Lesterlin C, Sherratt DJ (2011) Activation of XerCD-dif recombination by the FtsK DNA translocase. *Nucleic Acids Res* 39(12):5140–5148.
17. Das B, Bischerour J, Barre F-X (2011) VGJphi integration and excision mechanisms contribute to the genetic diversity of *Vibrio cholerae* epidemic strains. *Proc Natl Acad Sci USA* 108(6):2516–2521.
18. Hamilton HL, Domínguez NM, Schwartz KJ, Hackett KT, Dillard JP (2005) *Neisseria gonorrhoeae* secretes chromosomal DNA via a novel type IV secretion system. *Mol Microbiol* 55(6):1704–1721.
19. Chen C-C, et al. (2011) Draft genome sequence of a dominant, multidrug-resistant *Neisseria gonorrhoeae* strain, TCDC-NG08107, from a sexual group at high risk of acquiring human immunodeficiency virus infection and syphilis. *J Bacteriol* 193(7):1788–1789.
20. Blakely GW, Davidson AO, Sherratt DJ (1997) Binding and cleavage of nicked substrates by site-specific recombinases XerC and XerD. *J Mol Biol* 265(1):30–39.
21. Diagne CT, et al. (2014) TPM analyses reveal that FtsK contributes both to the assembly and the activation of the XerCD-*dif* recombination synapse. *Nucleic Acids Res* 42(3):1721–1732.
22. Plénat T, Tardin C, Rousseau P, Salomé L (2012) High-throughput single-molecule analysis of DNA-protein interactions by tethered particle motion. *Nucleic Acids Res* 40(12):e89.
23. Manghi M, et al. (2010) Probing DNA conformational changes with high temporal resolution by tethered particle motion. *Phys Biol* 7(4):046003.
24. Crozat E, et al. (2010) Separating speed and ability to displace roadblocks during DNA translocation by FtsK. *EMBO J* 29(8):1423–1433.
25. May PFJ, Zawadzki P, Sherratt DJ, Kapanidis AN, Arciszewska LK (2015) Assembly, translocation, and activation of XerCD-*dif* recombination by FtsK translocase analyzed in real-time by FRET and two-color tethered fluorophore motion. *Proc Natl Acad Sci USA* 112(37):E5133–E5141.
26. Yates J, Aroyo M, Sherratt DJ, Barre F-X (2003) Species specificity in the activation of Xer recombination at *dif* by FtsK. *Mol Microbiol* 49(1):241–249.
27. Kono N, Arakawa K, Tomita M (2011) Comprehensive prediction of chromosome dimer resolution sites in bacterial genomes. *BMC Genomics* 12(1):19.
28. Carnoy C, Roten C-A (2009) The *dif*/Xer recombination systems in proteobacteria. *PLoS One* 4(9):e6531.
29. Graham JE, Sherratt DJ, Szczelkun MD (2010) Sequence-specific assembly of FtsK hexamers establishes directional translocation on DNA. *Proc Natl Acad Sci USA* 107(47):20263–20268.
30. Bigot S, Corre J, Louarn J-M, Cornet F, Barre F-X (2004) FtsK activities in Xer recombination, DNA mobilization and cell division involve overlapping and separate domains of the protein. *Mol Microbiol* 54(4):876–886.
31. Cornet F, Louarn J, Patte J, Louarn JM (1996) Restriction of the activity of the recombination site dif to a small zone of the *Escherichia coli* chromosome. *Genes Dev* 10(9):1152–1161.
32. Nolivos S, Pages C, Rousseau P, Le Bourgeois P, Cornet F (2010) Are two better than one? Analysis of an FtsK/Xer recombination system that uses a single recombinase. *Nucleic Acids Res* 38(19):6477–6489.
33. Brunet A, et al. (2015) Probing a label-free local bend in DNA by single molecule tethered particle motion. *Nucleic Acids Res* 43(11):e72.
34. Vanhooff V, Normand C, Galloy C, Segall AM, Hallet B (2010) Control of directionality in the DNA strand-exchange reaction catalysed by the tyrosine recombinase TnpI. *Nucleic Acids Res* 38(6):2044–2056.